Heat Transfer of Magnetohydrodynamic Generalized Power Law Blood Flow with Gold-Nanoparticles in a Stenosed Artery

Kannigah a/p Thirunanasambantham
Department of Mathematical Sciences, Faculty of Science, Universiti Teknologi Malaysia

Zuhaila Ismail
Department of Mathematical Sciences, Faculty of Science, Universiti Teknologi Malaysia

Lim Yeou Jiann
Department of Mathematical Sciences, Faculty of Science, Universiti Teknologi Malaysia

Amnani Shamjuddin
Chemical Reaction Engineering Group (CREG), Faculty of Chemical and Energy Engineering, Universiti Teknologi Malaysia

https://doi.org/10.5109/7395673

出版情報：Proceedings of International Exchange and Innovation Conference on Engineering & Sciences (IEICES). 11, pp.1264-1270, 2025-10-30. International Exchange and Innovation Conference on Engineering & Sciences
バージョン：

Heat Transfer of Magnetohydrodynamic Generalized Power Law Blood Flow with Gold-Nanoparticles in a Stenosed Artery

Kannigah a/p Thirunanasambantham[1], Zuhaila Ismail[1], Lim Yeou Jiann[1] , Amnani Shamjuddin[2],
[1] Department of Mathematical Sciences, Faculty of Science, Universiti Teknologi Malaysia, [2] Chemical Reaction Engineering Group (CREG), Faculty of Chemical and Energy Engineering, Universiti Teknologi Malaysia.
zuhaila@utm.my

Abstract: *The objective of this study is to analyse the heat transfer characteristics of magnetohydrodynamic generalised power-law blood flow containing gold nanoparticles in a stenosed artery. Four different stages of stenosis progression are considered. The heat transfer mechanism influenced by a magnetic field and Joule heating in a stenosed artery is crucial for both magnetic and hyperthermia treatments. Therefore, improving the effectiveness of these treatments is of paramount importance. Due to the high cost and complexity of experimental procedures, as well as ethical concerns related to human rights, this study is conducted theoretically. A mathematical model of blood flow is developed by simulating blood as a non-Newtonian fluid based on the generalised power-law model. The governing equations, along with appropriate boundary conditions, are solved using COMSOL software. Results related to velocity, temperature, and streamline patterns are analysed and discussed. Significant differences are observed in heat transfer with and without gold nanoparticles, and the application of a magnetic field and Au is able to reduce the arterial temperature by 35%. Large recirculations are observed when the stenosis is axisymmetric, and with the application of Au and a magnetic field, the flow recirculations are stabilised. By providing deeper insights into the fluid dynamics of arteries affected by progressive stenosis, this study contributes to the development of more effective treatment strategies.*

Keywords: Magnetohydrodynamic; Joule heating; Nanofluid; Stenosis; Generalized Power Law

1. INTRODUCTION

Extensive research on the hemodynamic characteristics of blood flow in stenotic vessels, particularly involving multiple stenoses, needs to be explored in order to understand the pathological mechanisms and reduce the incidence of stenosis. Stenosis refers to the narrowing of blood vessels, impedes blood flow, and can lead to blood clots or 'vulnerable plaques', increasing the risk of cardiovascular diseases (CAD) like stroke and heart attack [1], [2]. It is common for patients to be diagnosed with multiple types of stenosis in the same segment of an artery [3], [4]. Overlapping stenoses create complex flow patterns and low-shear stress regions conducive to new stenotic lesions. This cycle of vascular damage and narrowing often worsens in areas with existing stenosis, highlighting the need to study overlapping stenoses with a progressing new cosine-shaped stenosis for a more accurate understanding of physiological conditions in diseased arteries.

The accumulation of cholesterol, lipids, and smooth muscle cells in blood vessels leads to stenosis [5]. The excessive buildup of these substances can alter the rheological properties of blood. Therefore, it is essential to consider a non-Newtonian fluid model when analysing blood flow in such conditions. Blood exhibits shear-thinning properties, where the viscosity decreases with increasing shear strain, unlike Newtonian fluids. This behaviour becomes particularly evident in low-shear regions, where red blood cells clump together, forming larger particles and increasing viscosity [6], [7]. The generalised power-law model (GPL), recognised for its ability to combine various classical models, is widely accepted as the most accurate representation of blood's non-Newtonian characteristics [8]. According to Ikbal et al. [9], the GPL model is the most comprehensive non-Newtonian model because it combines various properties of classical models, making it suitable for representing the complex behaviour of blood. This support is further reinforced by Sharma et al., [10], who highlights that the GPL model effectively captures the non-Newtonian characteristics of blood by integrating several generalised classical models. Lakzian et al., [7] found that the GPL model provides a more accurate approximation of WSS, particularly under low-shear conditions.

Incorporating nanoparticles (NPs) into blood flow analysis further enhances its realism, as NPs can significantly alter the thermal and rheological properties of the fluid. These particles improve heat transfer, which is beneficial in medical applications like hyperthermia treatment [8]. Theoretical studies, such as those by Priyadharshini et al. [5] and Alghamdi et al. [11] highlight the significant impact of gold NPs (Au NPs) on blood flow and their potential in cardiovascular treatments. Au NPs, with their high surface area and biocompatibility, are particularly useful as drug delivery vehicles, enabling targeted therapy that reduces side effects and enhances treatment efficiency [5]. According to the study by Tayebi et al. [12], the presence of Au NPs, a magnetic field, and yield stress leads to an increased radius of the plug core in blood flow. The NPs aid in distributing heat more evenly, improving heat transfer efficiency, which can reduce localised overheating and improve the thermal environment within the artery [13]. This, in turn, may help slow the progression of stenosis. The findings suggest that incorporating Au NPs in blood flow analysis could lead to improved diagnostic techniques for CAD, enabling earlier detection and more personalised treatment strategies.

Magnetohydrodynamic (MHD) approaches provide a promising method for managing stenosis by leveraging magnetic fields to influence blood flow. The interaction between magnetic fields and the conductive properties of blood can alter hemodynamic characteristics, such as reducing bleeding during surgery, accelerating fracture healing, and mitigating depression symptoms [14]. Studies, including Zaperi *et al.,* [15], have shown that applying MHD decreases wall shear stress (WSS) at the extremities of an overlapping stenosis throat. Zain et al.[16] also considered MHD in a bifurcated artery by analysing the blood flow using the GPL model, and the results revealed that the presence of MHD was able to stabilise the erratic flow in the artery curvature. Additionally, the interaction between the magnetic field and electric current generates localised heating in arteries, emphasising the need to account for the Joule heating effect when analysing blood flow dynamics under MHD conditions.

The additional heat from the Joule heating effect plays a critical role in thermal therapy. An investigation by Sharma et al. [14] was conducted to investigate the effects of Joule heating and MHD on a convective nanofluid in a vertical plate. The study found that nanofluid thermal conductivity is significantly higher when Joule heating is applied. Ramesh et al. [17] examined the heat transfer within MHD peristaltic blood flow under the influence of the hall effect. A study conducted by Bhatti et al. [18] considered the Joule heating effect when delivering magnetic drugs through a tapered stenosed artery. The results of these studies indicated a noticeable increase in temperature homogeneously when the Joule heating parameter was increased. However, if blood under magnetisation degrades in a short period at temperatures exceeding 40 degrees, it can be life-threatening [5], [19].

Inspired by the aforementioned research, this study examines the heat transfer in blood flow over progressing stenosis with the application of the MHD and the Joule heating effect. This study is an extension of Zain *et al.,* [16], whereby considering the volume fraction of Au NPs and Joule heating. The main objective is to investigate the impact of four different types of stenosis on the blood flow with Au NPs while MHD and Joule's heating effect are considered. The fluid model is assumed to be a non-Newtonian GPL model. To simplify the underlying problem, the paper assumed mild stenosis for both overlapping and cosine-shaped stenosis. COMSOL Multiphysics, a software based on the finite element method (FEM), is used to obtain numerical results of flow due to the irregular geometry and small scale of stenoses.

The novelty of the present work:

- To analyse the fluid dynamics and heat transfer due to different stenosis progression.
- To study the impact of Joule heating and NPs on heat transfer of blood flow through a stenosed artery

2. MATHEMATICAL FORMULATION

Here are the assumptions imposed in formulating the computational domain of the stenosed artery:

- There is a mild stenosis, which progresses to an overlapping stenosis, classified into four types.
- The stenosis formed is assumed to be a cosine-shaped stenosis.

The geometry is constructed based on Zain et al. [16] and Xenos et al. [20]. In this study, the stenosis is considered at a mild artery, as shown in Fig. 1. Let (x, y) be the coordinates of a material point where the x-axis is taken along the axis of the trunk while the y-axis is taken along the y-direction. The geometry of the stenosed artery is presented by the following equation [16].

$$S_1(x)=\begin{cases} a, & 0<x<d \text{ and } l_1 \le x \le l_0 \\ a+\dfrac{4\delta}{l_1}\left\{l_1(x-d)-(x-d)^2\right\} & d \le x \le d+l_1 \end{cases}$$

$$S_2(x)=\begin{cases} a, & 0<x<d \text{ and } l_2 \le x \le l_0 \\ a-\dfrac{3\delta}{2l_2^4}\begin{bmatrix} 11(x-d)l_2^3-47(x-d)^2 l_2^2 \\ +72(x-d)^3 l_2-36(x-d) \end{bmatrix} & d \le x \le d+l_2 \end{cases} \quad (1)$$

where $S_1(x)$ (Progression 1) and $S_2(x)$ (Progression 2) are the radii of the cosine-shaped and multi-stenosis artery walls, respectively [19]. a is defined as the radius of the artery, l_0, l_1, and l_2 represent the length of the finite length of the artery, length of the cosine-shaped stenosis, and overlapping stenosis, respectively. The parameters d denote the length of the artery from the inflow. The occlusion of the stenosis for both overlapping and cosine-shaped is labelled as δ. The depth δ of the overlapping stenosis is maintained at (δ =0.25) [20], where Progression 1 forms cosine-shaped stenosis, Progression 2 develops overlapping stenosis, Progression 3 is axisymmetric cosine-shaped stenosis ($-S_1(x)$ and $S_1(x)$), and Progression 4 ($-S_2(x)$ and $S_2(x)$) is axisymmetric multi stenosis, (see Fig. 1).

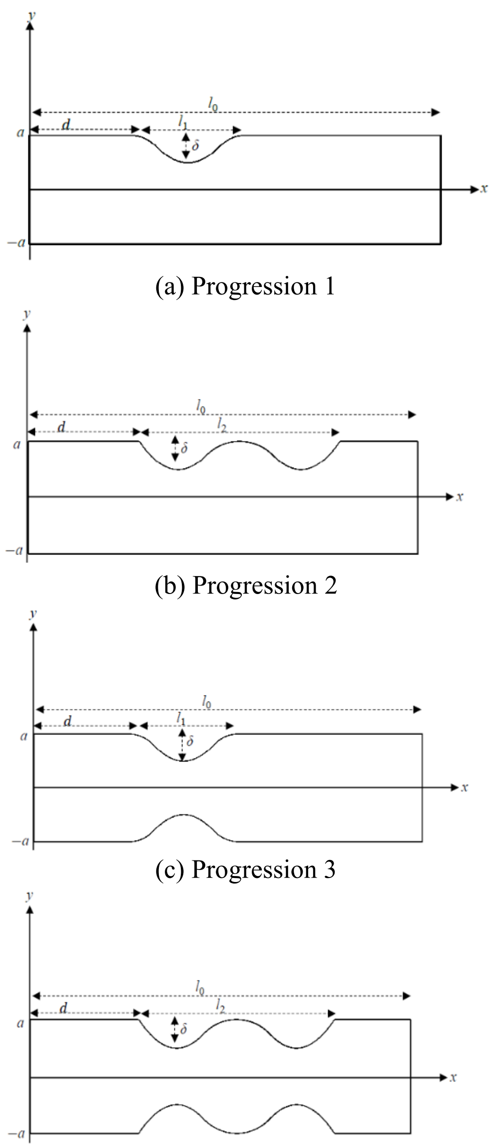

(a) Progression 1

(b) Progression 2

(c) Progression 3

(d) Progression 4

Fig. 1. Geometry model of each progression.

The fluid model in this study is considered to be in two-dimensional, laminar, steady, incompressible, and fully developed flow, where the blood is rheologically characterised as a non-Newtonian GPL. The blood flow is subjected to a uniform magnetic field with the effects of Joule heating and the addition of Au NPs. The dimensionless continuity, momentum, and energy equation of the flow can be written as [15,19]

$$\frac{\partial u}{\partial x}+\frac{\partial v}{\partial y}=0, \tag{2}$$

$$u\frac{\partial u}{\partial x}+v\frac{\partial u}{\partial y}=-\frac{\partial p}{\partial x}+\frac{1}{\mathrm{Re}}\left(\frac{\rho_f}{\rho_{nf}}\right)\left\{\left|\left[2\left(\frac{\partial u}{\partial x}\right)^2+2\left(\frac{\partial v}{\partial y}\right)^2+\left(\frac{\partial v}{\partial x}+\frac{\partial u}{\partial y}\right)^2\right]^{1/2}\right|^{n-1}\right\}\left(\frac{\partial^2 u}{\partial x^2}+\frac{\partial^2 u}{\partial y^2}\right)-\frac{M^2}{\mathrm{Re}}\left(\frac{\sigma_{nf}}{\sigma_f}\right)\left(\frac{\rho_f}{\rho_{nf}}\right)u, \tag{3}$$

$$u\frac{\partial v}{\partial x}+v\frac{\partial v}{\partial y}=-\frac{\partial p}{\partial y}+\frac{1}{\mathrm{Re}}\left(\frac{\rho_f}{\rho_{nf}}\right)\left\{\left|\left[2\left(\frac{\partial u}{\partial x}\right)^2+2\left(\frac{\partial v}{\partial y}\right)^2+\left(\frac{\partial v}{\partial x}+\frac{\partial u}{\partial y}\right)^2\right]^{1/2}\right|^{n-1}\right\}\left(\frac{\partial^2 v}{\partial x^2}+\frac{\partial^2 v}{\partial y^2}\right). \tag{4}$$

$$u\frac{\partial T}{\partial x}+v\frac{\partial T}{\partial y}=\mathrm{Pr}\,\mathrm{Re}\left(\frac{k_{nf}}{k_f}\right)\left(\frac{(\rho c_p)_f}{(\rho c_p)_{nf}}\right)\left(\frac{\partial^2 T}{\partial x^2}+\frac{\partial^2 T}{\partial y^2}\right)+\mathrm{Br}M^2u^2\left(\frac{(\rho c_p)_f}{(\rho c_p)_{nf}}\right) \tag{5}$$

where the term $-\frac{M^2}{\mathrm{Re}}\left(\frac{\sigma_{nf}}{\sigma_f}\right)\left(\frac{\rho_f}{\rho_{nf}}\right)$ are the Loretz force. Term $\mathrm{Br}M^2u^2\left(\frac{(\rho c_p)_f}{(\rho c_p)_{nf}}\right)$ in Eq. (4) represent the Joule heating effect. Reynolds number (Re), Hartmann number (M), Prandtl number (Pr), Brinkmann number (Br), and Eckert number (Ec) are defined as [21]

$$\mathrm{Re}=\frac{\rho_f h}{mU_0^{n-2}},\ M=B_0\left(\frac{\sigma_f h^{n+1}}{mU_0^{n-1}}\right)^{1/2},\ \mathrm{Ec}=\frac{U_0^{\,2}}{\left((T_1-T_0)+T_0\right)c_{p,f}}$$
$$\mathrm{Pr}=\frac{mc_{p,f}h^{1-n}}{k_f U_0^{\,1-n}}\ \text{ and }\ \mathrm{Br}=\mathrm{Ec}\,\mathrm{Pr} \tag{6}$$

where u and v are the velocities of blood in the x and y directions, respectively. The dimensional variable h is the length of the artery inlet, and U_0 is the reference velocity. Subscripts f and nf represent fluid and nanofluid, respectively; hence, ρ_f and ρ_{nf} implies the density of blood and nanofluid, respectively. Similarly, this applies to k_f and k_{nf} which are thermal conductivity, $(\rho c_p)_f$, and $(\rho c_p)_{nf}$ which are the heat capacity and σ_f and σ_{nf} which are the electrical conductivity of fluid and nanofluid, respectively. p is defined as pressure, m represents the fluid consistency, and n is the power law index, which, in this case, n=1.2 is assumed to classify blood as shear-thickening fluid to represent the GPL model.

At the inlet of the artery, a parabolic velocity profile is assumed, following the assumptions made, where fully developed flow [16], which is given by

$$u(0,y)=1-\left(\frac{y^2}{a^2}\right),\ v(0,y)=0,\ \ and\ -a<y<a, \tag{7}$$

At the outlet of the artery, a traction-free condition with no tangential and normal forces was applied [16], written as

$$(-p\mathbf{I}+\tau)\mathbf{n}=0\,, \tag{8}$$

where **I** is the unit tensor and **n** is the unit outward normal vector. Along the wall of the artery, the no-slip condition is applied [16],

$$u(x,y)=0,\ v(x,y)=0, \tag{9}$$

The temperature of the artery wall is prescribed as [22]

$$T_0(x,y)=1 \text{ along the arterial wall and } T_1(x,y)=0 \text{ at the inlet.} \tag{10}$$

This condition reflects a realistic physiological scenario where blood enters the artery at body temperature and is then heated by external sources such as magnetic fields or Joule heating [22]. The condition $T_1 < T_0$ ensures that heat flows from the arterial wall into the bloodstream, which is essential for simulating thermal therapies or localised heating treatments [22].

2.1 Computational Mesh and Validation

In order to verify the validity of these results and ensure they were not dependent on mesh parameters, we performed computational validation and a mesh dependency test using the computational domain demonstrated in Fig. 2 as given in [20]. While the mathematical formulation and governing equations in this study are presented in dimensionless form to generalise the analysis and reduce parameter complexity, dimensional quantities are reintroduced in the computational mesh and validation section to enable direct comparison with previous numerical study. Parameters like artery height h, which was used in the non-dimensionalisation process, are now expressed in their original dimensional form to match the reference geometry and validate the model against established results. By considering blood flow as a Newtonian fluid and applying magnetisation parameters B of 0T, 8T, 16T, and 32T, the computed solutions are validated with [20]. Table 1 summarises the number of domain elements and maximum velocity, U_{max}. According to Table 1, the current maximum velocity results and Xenos *et al.,* [20] agreed well with each, especially (Mesh 3 and Mesh 4), with a very small difference recorded, approximately 0.009 m/s. There may be slight differences as a result of flow unsteadiness and different validation methods. In order to reduce computational time, Mesh 3 is selected in order to provide a satisfactory solution to our problem.

Table 1
Comparison of various meshes with different magnetic parameters B

Mesh	Domain elements	U_{max}			
		B			
		0T	8T	16T	32T
1	3744	1.569	1.488	1.461	1.426
2	6678	1.586	1.499	1.470	1.428
3	16306	1.592	1.517	1.486	1.440
4	39370	1.595	1.522	1.489	1.453
Xenos et al. [20]		1.586	1.524	1.494	1.457

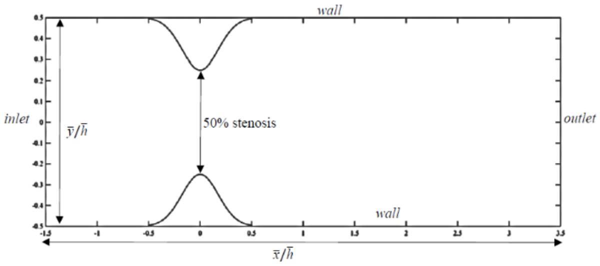

Fig.2 Straight rectangular channel with bell-shaped stenosis [20].

3. RESULTS AND DISCUSSION

Detailed analysis of the behaviour of fluid flow in terms of streamline, velocity, and temperature gradient is done on each progression of stenosis. The streamline velocity and maximum velocity of each progression are illustrated (see Fig. 3) to show how the fluid flows and heat transfers as the stenosis progresses without MHD and the presence of Au NPs. Fig. 3(a) illustrates the cosine-shaped stenosis where the large flow stagnation is formed at the post-stenotic region. As the stenosis progresses to Fig 3(b), the velocity increases with two regions of flow recirculation at the post-stenotic region. This flow recirculation worsens as the progression increases (see Fig. 3(c) and (d)), forming two large flow stagnations at the outlet part of the artery. It is evident that this phenomenon causes the fluid flow to slow down or become stationary, hence forming regions of low velocity and reversal of flow. As the progression of the stenosis increases, these recirculation zones become more pronounced and increase pressure due to the prolonged residence time of the fluid in these areas. The altered flow dynamics can also lead to increased turbulence, and temperature in the vicinity of the stenosis can further compromise the vascular integrity, leading to a cycle of progressive narrowing and increased stenosis severity [22]. This can ultimately result in more significant blockages and a higher risk of adverse clinical outcomes [23].

The streamline and maximum velocity during stenosis progression with M=20 and Au NPs are shown in Fig. 4. Fig. 4(a) depicts smooth blood flow with low velocity at the stenosis center compared to Fig. 3(a). As stenosis progresses in Fig. 4(b), velocity remains low due to MHD and Au NPs, with stable flow and no stagnation at the post-stenotic region. However, in Fig. 4(c) and (d), flow recirculation is formed but smaller and smoother. MHD and Au NPs controlled and reduced maximum velocity compared to Fig. 3(c) and (d), but the magnetic field is insufficient to eliminate flow stagnations. Overall, the addition of MHD and Au NPs enhanced the velocity profile and reduced flow resistance, leading to improved hemodynamic performance in all types of geometry, like single, multiple, and also axisymmetric stenoses.

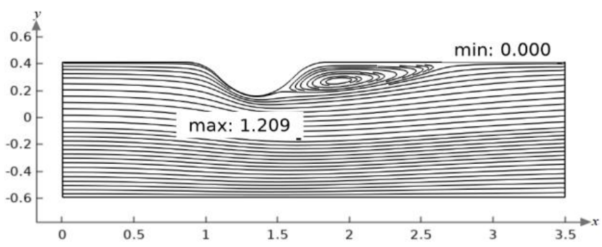

(a) Progression 1

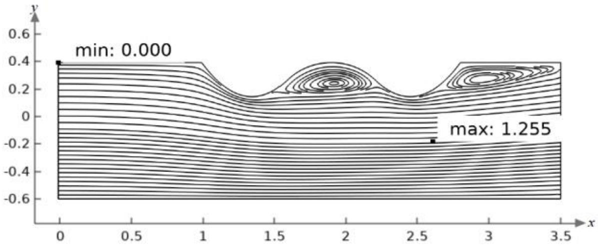

(b) Progression 2

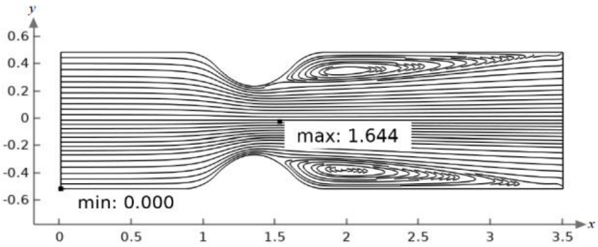

(c) Progression 3

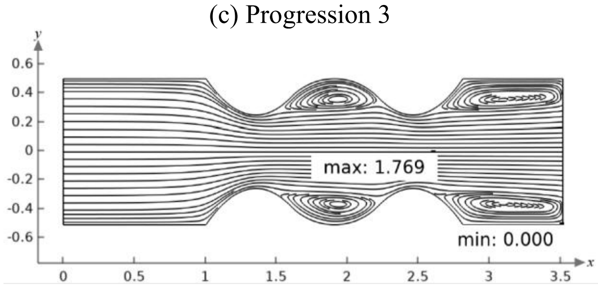

(d) Progression 4

Fig. 3. Streamline velocity of each progression without MHD and Au NPs.

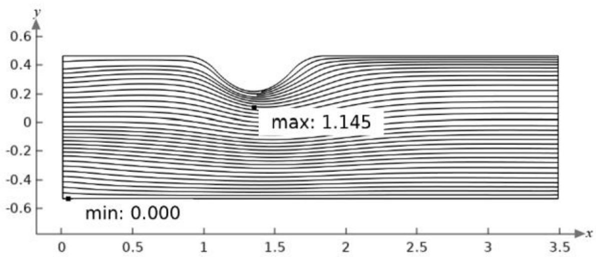

(a) Progression 1

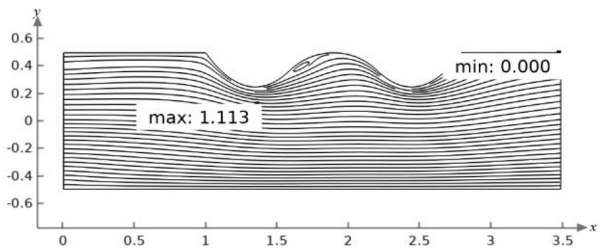

(b) Progression 2

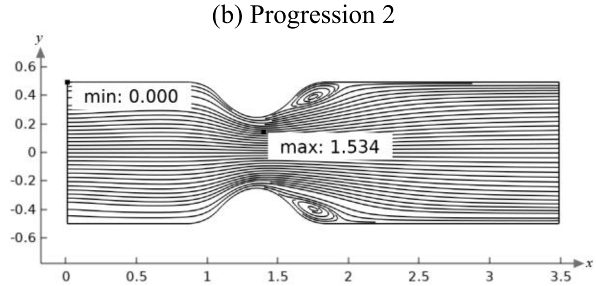

(c) Progression 3

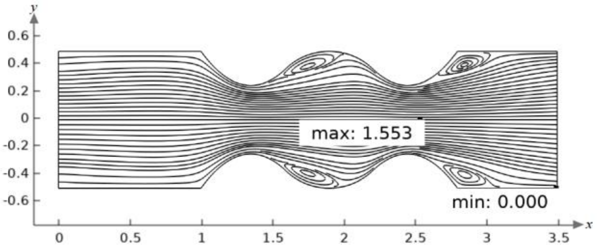

(d) Progression 4

Fig. 4. Streamline velocity of each progression with MHD and Au NPs.

The velocity profile with varying magnetic field parameters M with and without Au NPs in each stage of stenosis progression is depicted in Fig. 5. The magnetic field is varied into four values (M=0, M=13, M=20, and M=36), and the volume fraction of Au NPs is set at 0.01. The velocity trendline is analysed at x = 2.8, which is at the post-stenotic region because it often exhibits maximum velocity [11]. This choice allows for a comprehensive analysis of fluid behaviour in this area [11].

Overall, based on Fig. 5, the velocity increases as the progression worsens. As stenosis progresses from 1 to 4, the narrowing of the vessel results in a reduction of the cross-sectional area through which the fluid can flow. This constriction causes the fluid velocity to increase in order to maintain the same volumetric flow rate, as dictated by the principle of continuity. Fig. 5(a) shows the velocity with only one peak where the stenosis is located. The velocity is very high with a presence of flow stagnation at the post-stenotic region without the MHD. However, with increasing M, the velocity decreases across Fig. 5(a),(b),(c), and (d). It is physically justified that the fluid experiences a resistive force as the magnetic field strength increases. The blood flow contains haemoglobins, which affect the flow due to its interaction with the magnetic field, leading to a decrease in fluid velocity [9].

On top of that, as the severity of the stenosis forms asymmetrically, the presence of the Au NPs in blood flow increases viscosity and thermal conductivity then, enhancing momentum transfer and creating a smoother, more parabolic flow, as shown in Fig. 5(a),(b),(c), and (d). As the blood flows along the wall, the velocity profile reduces more than without Au NPs. This phenomenon is able to reduce plaque buildup and lower the risk of rupture. Au NPs also increase drag forces, further decreasing velocity near arterial walls. This trendline from Fig. 5(c) and (d) indicates that as the severity of stenosis increases, the application of MHD with Au NPs, especially the value of (M=20 and M=36), effectively reduces the velocity remarkably at the post-stenotic region, illustrating the efficacy in managing blood flow dynamics.

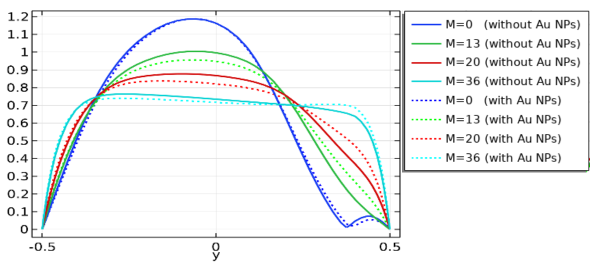

(a) Progression 1

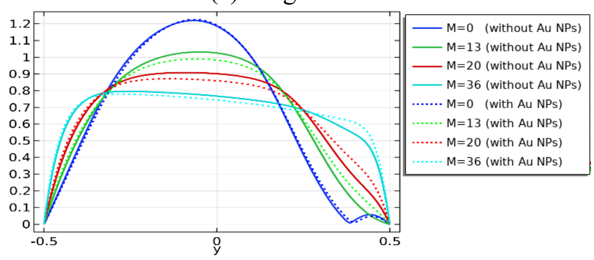

(b) Progression 2

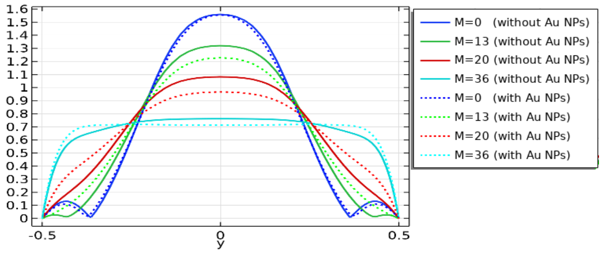

(c) Progression 3

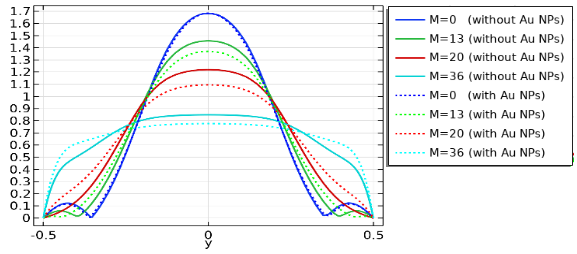

(d) Progression 4

Fig. 5. Velocity profile of each progression with and without Au NP.

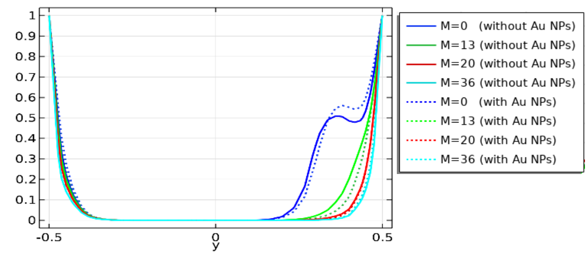

(a) Progression 1

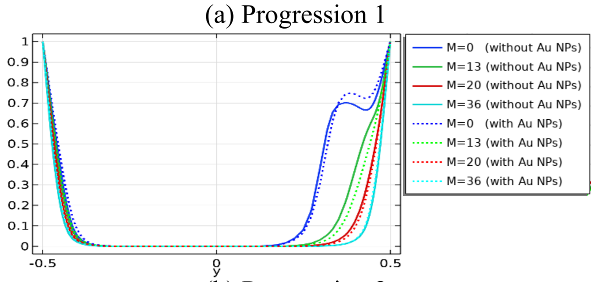

(b) Progression 2

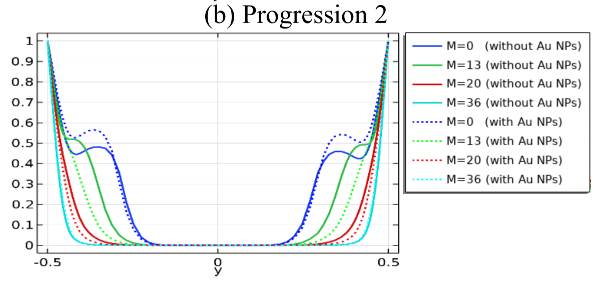

(c) Progression 3

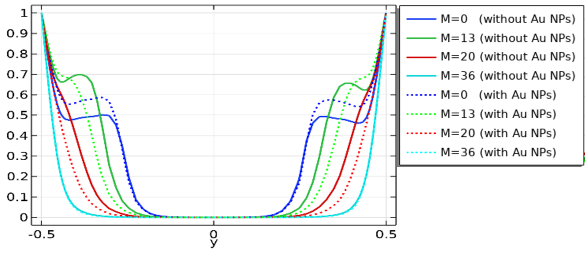

(d) Progression 4

Fig. 6. Temperature gradient of each progression with and without Au NP.

Fig. 6 illustrates the temperature profile with increasing M values with and without the presence of Au NPs with different stenosis progression at the post-stenotic region (x=2.8). As the stenosis constricts asymmetrically (see Fig. 6(c) and (d)), double temperature peaks are observed in the post-stenotic region compared to single peaks in Fig. 6(a) and (b). At M=0, distinct temperature peaks occur due to the absence of MHD, allowing natural variations in temperature to manifest prominently (see Fig. 6). These peaks arise because, without MHD, fluid flow and heat distribution are less controlled, leading to higher temperature differences at the boundaries of the stenosis [9]. However, when M=0, the heat transfer with Au NPs is lower compared to without Au NPs. This occurs because, without the stabilising effect of the MHD, the Au NPs can cause increased viscosity and resistance near the arterial walls, reducing the overall heat transfer [18].

As the M increases, the magnetic field exerts a stabilising effect on the fluid flow, resulting in a more uniform temperature distribution. At M=13, the MHD influence is moderate, partially stabilising the flow but not strong enough to completely counteract the effects of severe stenosis, leading to localised temperature peaks. The addition of Au NPs further influences the heat transfer dynamics. The temperature profile with Au NPs increases with increasing M. This is because Au NPs enhance the thermal conductivity of the blood, improving heat transfer efficiency. This stabilisation is achieved as the MHD aligns the NPs and haemoglobins, reducing temperature fluctuations [17]. The enhanced heat transfer due to NPs also aids in dissipating heat more effectively, which can prevent overheating and potential damage to the arterial walls. However, as the magnetic parameter M increases further (e.g., M=20 and M=36), the magnetic field exerts a stronger stabilising effect on the fluid flow, reducing temperature fluctuations caused by variations in stenosis severity. This results in a more uniform temperature distribution. It is also noteworthy that when M=36, the temperature profiles with and without Au NPs are the same due to the dominant influence of the MHD. At such a high M value, the MHD exerts a strong stabilising effect on the fluid flow, leading to a uniform temperature distribution throughout the artery [17]. In this scenario, the MHD's influence overrides the thermal enhancements provided by the Au NPs, resulting in similar temperature profiles regardless of their presence.

The effect of Joule heating is more pronounced at higher values of M, where the magnetic field interacts more strongly with the fluid, generating heat and contributing to the temperature distribution. Joule heating is more significant in the post-stenotic region, where there are peaks indicating regions with substantial heat generation. For low-severity stenosis, increasing M results in smoother flow profiles without significant peaks. For high-severity stenosis, higher M values still show inconsistencies due to severe geometric constraints despite strong magnetic stabilisation. While higher M values provide better stabilisation, they may not fully counteract severe geometric disruptions. Lower M values are less effective at stabilisation but sufficient for mild cases, avoiding excessive thermal buildup from Joule heating. With Au NPs and MHD, the increased thermal conductivity helps to dissipate the heat generated by Joule heating more efficiently and reduce high temperatures by 35%, reducing the risk of localised overheating. Without Au NPs, the Joule heating effect can lead to higher localised temperatures, potentially causing more damage to the arterial walls [17].

4. CONCLUSION

This study analyses blood flow behavior in a progressing cosine-shaped stenosis and overlapping stenoses. The mathematical model incorporates MHD, Au NPs, and considers blood as GPL fluid while accounting for Joule heating. Key findings include:

- Flow stagnation and recirculation increase as stenosis progresses, impacting the development of atherosclerosis.
- Velocity decreases smoothly with increasing M, stabilising fluid flow in intricate regions. The presence of Au NPs further stabilises the velocity, especially in the post-stenotic regions.
- Temperature increases with stenosis severity, especially in the stenosed region.
- Temperature gradient decreases with increasing Hartman number M. The application of Au NPs increases the temperature slightly, indicating improved heat transfer efficiency

This comprehensive approach provides insights into the complex interactions affecting fluid dynamics in critical conditions. The research has significant potential for improving medical devices and therapies for cardiovascular conditions, enhancing patient outcomes, and reducing life-threatening events. Future studies could explore the effects of various NPs and extend the model to include permeable wall conditions for a more accurate representation of physiological scenarios.

5. ACKNOWLEDGMENT

This research was funded by the Universiti Teknologi Malaysia (UTM), UTM Fundamental Research Vote No: Q.J130000.3854.23H57 and Q.J130000.3854.23H02.

6. REFERENCES

[1] S. Nadeem, S. Akhtar, A. Saleem, N. Akkurt, H. Ali Ghazwani, and S. M. Eldin, “Numerical computations of blood flow through stenosed arteries via CFD tool OpenFOAM,” Alexandria Eng. J., vol. 69, pp. 613–637, 2023, doi: 10.1016/j.aej.2023.02.005.

[2] A. P. Sinica, “A Case of Metabolic Syndrome with Coronary Artery Disease Advanced over 13 Years." 1,3 (1,” Electron. Publ., vol. 96, no. 9, p. 250, 2005.

[3] N. M. Zain and Z. Ismail, “Numerical solution of magnetohydrodynamics effects on a generalised power law fluid model of blood flow through a bifurcated artery with an overlapping shaped stenosis,” PLoS One, vol. 18, no. 2 February, pp. 1–29, 2023, doi: 10.1371/journal.pone.0276576.

[4] Y. Sawayama, K. Okada, S. Maeda, H. Ohnishi, N.

Furusyo, and J. Hayashi, “Both hepatitis C virus and Chlamydia pneumoniae infection are related to the progression of carotid atherosclerosis in patients undergoing lipid lowering therapy.,” Fukuoka Igaku Zasshi, vol. 97, no. 8, pp. 245–255, 2006.
[5] S. Priyadharshini and R. Ponalagusamy, “Mathematical modelling for pulsatile flow of Casson fluid along with magnetic nanoparticles in a stenosed artery under external magnetic field and body acceleration,” Neural Comput. Appl., vol. 31, no. 3, pp. 813–826, 2019, doi: 10.1007/s00521-017-3111-8.
[6] M. Sharma, B. K. Sharma, U. Khanduri, N. K. Mishra, S. Noeiaghdam, and U. Fernandez-Gamiz, “Optimization of heat transfer nanofluid blood flow through a stenosed artery in the presence of Hall effect and hematocrit dependent viscosity,” Case Stud. Therm. Eng., vol. 47, no. April, p. 103075, 2023, doi: 10.1016/j.csite.2023.103075.
[7] E. Lakzian and P. Akbarzadeh, “Numerical investigation of unsteady pulsatile Newtonian/non-Newtonian blood flow through curved stenosed arteries,” Biomed. Mater. Eng., vol. 30, no. 5–6, pp. 525–540, 2020, doi: 10.3233/BME-191072.
[8] K. Kakavand, N. Koosha, K. Fathi, and S. Aminian, “Numerical investigation of capture efficiency of carrier particles in a Y-shaped vessel considering particle-particle interaction and Non-Newtonian behavior,” J. Drug Deliv. Sci. Technol., vol. 67, no. November 2021, p. 102997, 2022, doi: 10.1016/j.jddst.2021.102997.
[9] M. A. Ikbal, S. Chakravarty, K. K. L. Wong, J. Mazumdar, and P. K. Mandal, “Unsteady response of non-Newtonian blood flow through a stenosed artery in magnetic field,” J. Comput. Appl. Math., vol. 230, no. 1, pp. 243–259, 2009, doi: 10.1016/j.cam.2008.11.010.
[10] C. K. Bhupendra K. Sharma and M. M. Bhatti, “Optimizing energy generation in power-law nanofluid flow through curved arteries with gold nanoparticles,” Numer. Heat Transf. Part A Appl., vol. 0, no. 0, pp. 1–33, 2023, doi: 10.1080/10407782.2023.2232123.
[11] T. Gul et al., “Mixed convection stagnation point flow of the blood based hybrid nanofluid around a rotating sphere,” Sci. Rep., vol. 11, no. 1, pp. 1–15, 2021, doi: 10.1038/s41598-021-86868-x.
[12] T. Tayebi and A. J. Chamkha, “Entropy generation analysis due to MHD natural convection flow in a cavity occupied with hybrid nanofluid and equipped with a conducting hollow cylinder,” J. Therm. Anal. Calorim., vol. 139, no. 3, pp. 2165–2179, 2020, doi: 10.1007/s10973-019-08651-5.
[13] G. L. Santana, M. C. Crovace, E. E. Mazón, A. J. A. de Oliveira, T. Z. Pavan, and E. D. Zanotto, “Smart Bone Graft Composite for Cancer Therapy Using Magnetic Hyperthermia,” Materials (Basel)., vol. 15, no. 9, 2022, doi: 10.3390/ma15093187.
[14] R. P. Sharma, K. Badak, and S. R. Mishra, “Investigation of steady viscous magnetohydrodynamic copper–alumina/ethylene glycol hybrid nanofluid in mixed convective vicinity stagnation-point over a vertical plate with Joule heating,” J. Therm. Anal. Calorim., vol. 149, no. 10, pp. 4913–4924, 2024, doi: 10.1007/s10973-024-13050-6.
[15] N. H. A. Mohd Zaperi, N. A. Jaafar, and D. S. Sankar, “Solute Dispersion in Casson Blood Flow through a Stenosed Artery with the Effect of Temperature and Electric Field,” J. Adv. Res. Exp. Fluid Mech. Heat Transf., vol. 17, no. 1 SE-Articles, pp. 14–34, Sep. 2024, doi: 10.37934/arefmht.17.1.1434.
[16] N. M. Zain, Z. Ismail, and P. Johnston, “Numerical Analysis of Blood Flow Behaviour in a Constricted Porous Bifurcated Artery under the Influence of Magnetic Field,” CFD Lett., vol. 15, no. 1, pp. 39–58, 2023, doi: 10.37934/cfdl.15.1.3958.
[17] K. Ramesh, A. Riaz, and Z. A. Dar, “Simultaneous effects of MHD and Joule heating on the fundamental flows of a Casson liquid with slip boundaries,” Propuls. Power Res., vol. 10, no. 2, pp. 118–129, 2021, doi: 10.1016/j.jppr.2021.05.002.
[18] M. M. Bhatti, S. M. Sait, and R. Ellahi, “Magnetic Nanoparticles for Drug Delivery through Tapered Stenosed Artery with Blood Based Non-Newtonian Fluid,” Pharmaceuticals, vol. 15, no. 11, 2022, doi: 10.3390/ph15111352.
[19] N. M. Zain and Z. Ismail, “Dynamic Response of Heat Transfer in Magnetohydrodynamic Blood Flow Through a Porous Bifurcated Artery with Overlapping Stenosis,” J. Adv. Res. Fluid Mech. Therm. Sci., vol. 101, no. 1, pp. 215–235, 2023, doi: 10.37934/arfmts.101.1.215235.
[20] M. Xenos and E. Tzirtzilakis, “MHD Effects on Blood Flow in a Stenosis Department of Mathematics Technological Educational Institute of Western Greece,” no. May, 2016.
[21] C. Kumawat, B. K. Sharma, Q. M. Al-Mdallal, and M. Rahimi-Gorji, “Entropy generation for MHD two phase blood flow through a curved permeable artery having variable viscosity with heat and mass transfer,” Int. Commun. Heat Mass Transf., vol. 133, p. 105954, 2022, doi: https://doi.org/10.1016/j.icheatmasstransfer.2022.105954.
[22] Zuhaila Ismail, Muhammad Sabaruddin Ahmad Jamali, Norliza Mohd Zain, and Lim Yeou Jiann, “Bioheat transfer of Blood Flow on Healthy and Unhealthy Bifurcated Artery: Stenosis,” J. Adv. Res. Appl. Sci. Eng. Technol., vol. 28, no. 2, pp. 56–79, 2022, doi: 10.37934/araset.28.2.5679.
[23] S. O. Salawu, E. O. Fatunmbi, R. A. Kareem, O. M. Akinmoladun, and S. D. Ogundiran, “Radiating and Joule heating on heat and mass transfer of magnetized tiny particles in tangent hyperbolic nonlinear porosity flow with Riga plate and Arrhenius reaction,” Partial Differ. Equations Appl. Math., vol. 11, p. 100840, 2024, doi: https://doi.org/10.1016/j.padiff.2024.100840.

7